BMC Medical Imaging

RESEARCH

Open Access

A short-term predictive model for disease progression in acute-on-chronic liver failure: integrating spectral CT extracellular liver volume and clinical characteristics

Yuan Xu[1,2,3†], Fukai Li[4†], Bo Liu[5†], Tiezhu Ren[1,2,3], Jiachen Sun[1,2,3], Yufeng Li[1,2,3], Hong Liu[1,2,3], Jianli Liu[1,2,3*†] and Junlin Zhou[1,2,3*†]

Abstract

Background Acute-on-chronic liver failure (ACLF) is a life-threatening hepatic syndrome. Therefore, this study aimed to develop a comprehensive model combining extracellular liver volume derived from spectral CT ($ECV_{IC-liver}$) and sarcopenia, for the early prediction of short-term (90-day) disease progression in ACLF.

Materials and methods A retrospective cohort of 126 ACLF patients who underwent hepatic spectral CT scans was included. According to the Asia-Pacific Association for the Study of the Liver (APASL) criteria, patients were divided into the progression group ($n=70$) and the stable group ($n=56$). $ECV_{IC-liver}$ was measured on the equilibrium period (EP) images of spectral CT, and L3-SMI was measured on unenhanced CT images, with sarcopenia assessed. A comprehensive model was developed by combining independent predictors. Model performance was evaluated using receiver operating characteristic (ROC) curve analysis, calibration curves, and decision curve analysis (DCA).

Results In the univariate analysis, BMI, WBC, PLT, PTA, L3-SMI, IC-EP, Z-EP, K_{140}-EP, NIC-EP, $ECV_{IC-liver}$, and Sarcopenia demonstrated associations with disease progression status at 90 days in ACLF patients. In multivariate logistic regression, white blood cell count (WBC) (OR = 1.19, 95% *CI*: 1.02–1.40; $P=0.026$), $ECV_{IC-liver}$ (OR = 1.27, 95% *CI*: 1.15–1.40; $P<0.001$), sarcopenia (OR = 4.15, 95% *CI*: 1.43–12.01; $P=0.009$), MELD-Na score (OR = 1.06, 95%*CI*: 1.01–1.13;$P=0.042$), and CLIF-SOFA score (OR = 1.37, 95%*CI*:1.15–1.64; $P<0.001$) emerged as independent risk factors for ACLF progression. The combined model exhibited superior predictive performance (AUCs = 0.910, sensitivity = 80.4%, specificity = 90.0%, PPV = 0.865, NPV = 0.851) compared to CLIF-SOFA, MELD-Na, MELD and CTP scores(both $P<0.001$). Calibration curves and DCA confirmed the high clinical utility of the combined model.

†Yuan Xu, Fukai Li and Bo Liu contributed equally to this work.

†Jianli Liu and Junlin Zhou are co–senior authors.

*Correspondence:
Jianli Liu
liujl_1219@163.com
Junlin Zhou
ery_zhoujl@lzu.edu.cn

Full list of author information is available at the end of the article

Conclusions Patients without sarcopenia and/or with a lower $ECV_{IC-liver}$ have a better prognosis, and the integration of WBC, $ECV_{IC-liver}$, Sarcopenia, CLIF-SOFA and MELD-Na scores in a composite model offers a concise and effective tool for predicting disease progression in ACLF patients.

Trial registration Not Applicable.

Keywords Acute-on-chronic liver failure, Spectral CT, Extracellular liver volume, Sarcopenia, Combined model

Introduction

Acute-on-chronic liver failure (ACLF) represents a spectrum of clinical syndromes arising in the context of chronic liver disease, marked by multi-organ failure and a heightened risk of short-term mortality [1]. ACLF exhibits an exceptionally high 90-day adverse progression incidence, with reported mortality rates exceeding 50% in the Asia-Pacific region [2]. The condition poses significant diagnostic and therapeutic challenges due to its rapid onset, swift progression, heightened short-term mortality risk, and unfavorable prognosis [3, 4]. Prognostic evaluation for ACLF patients, particularly early assessments, is of paramount importance throughout clinical workup. This emphasis is crucial, aiming to facilitate timely considerations for liver transplantation (LT) whenever deemed feasible [5, 6].

The Model for End-Stage Liver Disease (MELD) and the MELD with Sodium (MELD-Na) stand as commonly utilized tools for prognostic assessment in liver disease. Despite their widespread use, both scoring systems lack parameters that specifically address the nuanced aspects of effective hepatic function and nutritional status in ACLF patients [7]. Considering the profound impact of hepatocyte function and systemic nutritional status on the severity of ACLF and its association with short-term mortality, the limitations of these conventional scoring models become apparent [8]. Large cohort studies have indicated an inherent tendency for the MELD score and MELD-Na score to underestimate the 3-month risk of death in ACLF patients [9, 10]. The Chronic Liver Failure-Sequential Organ Failure Assessment (CLIF-SOFA) score is a reliable scoring system for assessing liver and extrahepatic organ failure. Its ability to predict short-term mortality in ACLF has been confirmed by previous studies [11]. Adding to the complexity, the unique landscape of liver disease etiology in the Asia-Pacific region, primarily driven by hepatitis B virus (HBV) infection, distinguishes it from the Western counterparts, highlighting the need for prognostic scoring models tailored to the Chinese population [12]. Consequently, relying on the existing scoring models may hinder the provision of timely and accurate prognostic predictions for ACLF. In light of these considerations, there exists an urgent imperative for the development of a predictive model that can more precisely and comprehensively capture the short-term prognosis of ACLF patients.

As an innovative functional imaging modality, spectral CT stands out for its unique advantages in diagnosing, differentiating, and predicting the prognosis of advanced liver diseases. Notably, the extracellular liver volume (ECV), quantified through spectral CT, offers high reproducibility, intuitive visualization, and quantification. Specifically, ECV proves to be an efficient and noninvasive predictor of unfavorable disease progression in cirrhosis patients [13]. The efficacy of ECV in predicting poor disease progression can be attributed to its reflection of both the extent of collagen and matrix protein deposition in the extracellular interstitial space of the liver and, to some extent, the liver function itself [14]. Previous research from our team demonstrated that spectral CT-derived ECV effectively predicted short-term disease progression in patients with liver cirrhosis-acute decompensation [15]. However, prior investigations from our team primarily focused on liver function, overlooking the potential impact of nutritional status on the prognosis of patients with advanced liver disease.

Sarcopenia, a prevalent complication in advanced liver disease, serves as an effective indicator of overall nutritional status and has been consistently linked to the clinical outcomes of patients with acute-on-chronic liver failure (ACLF) [7, 16, 17]. Sarcopenia is indicative of a decline in skeletal muscle mass and function [18]. In patients with advanced liver disease, various factors, such as physical inactivity and ascites, contribute to reduced energy intake, excessive activation of muscle protein degradation, and impaired protein synthesis. These factors lead to progressive muscle wasting, which ultimately results in malnutrition (sarcopenia) [19]. A significant body of prior research has focused on the impact of sarcopenia in cirrhosis patients, demonstrating its strong prognostic value [20, 21]. However, given the differences in the onset and metabolic mechanisms between ACLF and cirrhosis, the prognostic significance of sarcopenia in ACLF remains to be further explored. Presently, CT measurement of skeletal muscle at the lumbar 3 vertebral level is a common method to assess whole-body skeletal muscle condition, with the L3-skeletal muscle index (SMI) widely adopted for defining sarcopenia [22]. Moreover, the L3-SMI obtained from non-contrast-enhanced liver CT scans is more easily applicable in clinical practice, as it can be simultaneously acquired during routine disease evaluation and follow-up CT scans without the

need for additional imaging [23]. Despite these advances, relying solely on clinical features and sarcopenia information for predicting poor prognosis in ACLF yields widely variable efficacy, with an area under the curve (AUC) range spanning from 0.636 to 0.865 [7, 24].

Therefore, the study aimed to create an integrated model by combining hepatic spectral CT-derived $ECV_{IC-liver}$ and unenhanced CT-assessed sarcopenia (defined by L3-SMI). This combined model was developed to predict the 90-day disease progression in patients with ACLF. The primary objective is to provide a streamlined and effective tool for guiding clinical decision-making and offering a more precise prognosis reference for individuals with ACLF.

Materials and methods

Patients

We conducted a retrospective analysis of individuals diagnosed with ACLF and treated at our institution from June 2019 to December 2022, meeting the Asian-Pacific Association for the Study of the Liver (APASL) criteria. Jaundice (serum bilirubin ≥ 5 mg/dL) and coagulation disorder (international normalized ratio (INR) ≥ 1.5 or prothrombin activity (PTA) < 40%) complicated by ascites and/or encephalopathy within 4 weeks [25]. Inclusion Criteria encompassed individuals who underwent liver spectral CT multiphase enhancement examinations within 1 week before and after ACLF diagnosis, aged between 18 and 80 years. Exclusion Criteria: (1) presence of malignant tumors in the liver or other body parts; (2) anatomical variations of liver blood vessels significantly impacting blood supply; (3) concomitant severe chronic extrahepatic diseases (e.g., chronic kidney disease, heart failure, respiratory failure); (4) history of surgical treatments for cirrhosis and portal hypertension (e.g., liver transplantation, splenectomy, TIPS, TACE); (5) poor-quality CT images affecting measurements; (6) incomplete clinical information or loss of follow-up visits. The final cohort included 126 ACLF patients, as depicted in the patient selection flow chart (Fig. 1).

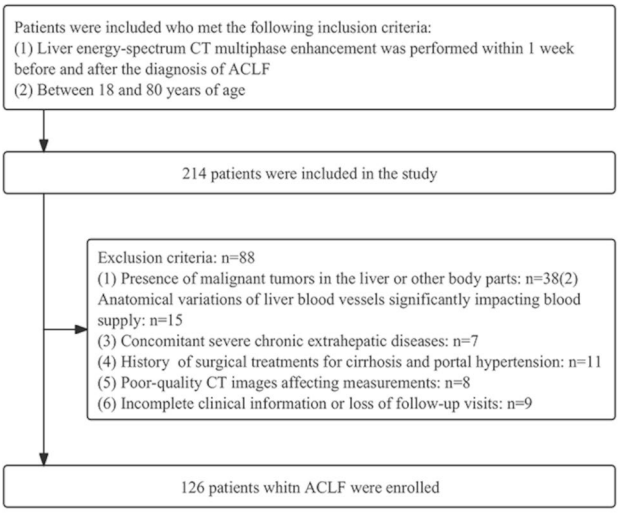

Fig. 1 Patient Selection Flowchart for Acute-on-Chronic Liver Failure (ACLF)

All patients diagnosed with ACLF underwent comprehensive medical management during hospitalization. This included etiological treatment, symptomatic care, and complication prevention strategies, such as smoking and alcohol cessation, antiviral therapy, discontinuation of drugs inducing liver injury, bed rest, plasma and albumin supplementation, hepatoprotective and anti-jaundice medications, water-electrolyte balance maintenance, nutritional support, and anti-inflammatory therapy. The study's primary endpoint was the 90-day progression status of ACLF patients, with follow-up conducted through a review of hospitalization records and/or telephone consultations. Patients discharged with improved or stable disease status within 90 days after ACLF diagnosis were categorized into the stable group, while those experiencing deterioration, death, or undergoing liver transplantation were classified into the progressive group.

The present study was approved by our hospital ethics committee (No. 2022 A-112) and performed according to the ethical guidelines of the 1975 Declaration of Helsinki. The requirement for obtaining informed consent from patients was waived because of the retrospective nature of the study.

Data collection

The clinical data for patients are summarized in Table 1, and prognostic scores, including the Child-Turcotte-Pugh (CTP) score, CTP classification, MELD score, MELD-Na score and CLIF-SOFA score, were computed utilizing the provided clinical information. The CLIF-SOFA score criteria are consistent with previous literature [26].

Calculation Formulas:

(1) CTP score and classification: The CTP score was the sum of the scores of five items (ascites, hepatic encephalopathy, TB, ALB, and PT extension time). The CTP score was classified as class A (5–6), class B (7–9), or class C (10–15) [27].

(2) MELD score = 3.8×Ln[TB (mg/dL)] + 11.2×Ln[INR] + 9.57×Ln[Cr (mg/dL)] + 6.43×etiology (0: alcoholic or cholestatic; 1: other).

(3) MELD-Na score = MELD + 1.59×[135-Na^+(mmol/L)]

Note Na^+ > 135 mmol/L is calculated as 135 mmol/L and Na^+ < 120 mmol/L is calculated as 120 mmol/L.

Table 1 Comparative analysis of clinical baseline characteristics in two groups of ACLF patients

Clinical Characteristics	Progressive Group (*n* = 70)	Stable Group (*n* = 56)	T/U/ c^2	*P* Value
Age (years)	51.0 ± 10.7	49.3 ± 9.9	-0.944	0.347
Gender, *n* (%)			0.002	0.968
male	41 (58.6%)	33 (58.9%)		
female	29 (41.4%)	23 (41.1%)		
BMI (kg/m^2)	22.9 (20.6, 26.7)	24.1 (22.9, 26.2)	-2.283	**0.022**
Etiology, *n* (%)			3.605	0.462
HBV	45 (64.3%)	37 (66.1%)		
HCV	7 (10.0%)	2 (3.6%)		
Alcohol	5 (7.1%)	3 (5.4%)		
Autoimmune/Biliary	7 (10.0%)	10 (17.9%)		
Others	6 (8.6%)	4 (7.1%)		
Infections, *n* (%)			1.639	0.200
Yes	62 (88.6%)	45 (80.4%)		
No	8 (11.4%)	11 (19.6%)		
Gastrointestinal bleeding, *n* (%)			0.411	0.521
Yes	13 (18.6%)	8 (14.3%)		
No	57 (81.4%)	48 (85.7%)		
Ascites, *n* (%)			1.646	0.200
Yes	61 (87.1%)	44 (78.6%)		
No	9 (12.9%)	12 (21.4%)		
Hepatic encephalopathy, *n* (%)			1.012	0.314
Yes	18 (25.7%)	19 (33.9%)		
No	52 (74.3%)	37 (66.1%)		
Sarcopenia, *n* (%)			11.421	**0.001**
Yes	37 (52.9%)	13 (23.2%)		
No	33 (47.1%)	43 (76.8%)		
BUN (mmol/L)	5.5 (4.1, 7.9)	5.25 (4.1, 6.5)	-0.791	0.429
Cr (umol/L)	69.5 (61.0, 76.2)	66.7 (52.2, 80.7)	-0.589	0.556
Na^+ (mmol/L)	137.4 (133.5, 139.3)	134.8 (131.4, 139.0)	-1.302	0.193
ALT (U/L)	39.5 (26.0, 56.3)	33.5 (17.8, 64.5)	-1.481	0.139
AST (U/L)	69.0 (44.3, 103.25)	62.0 (32.5, 121.0)	-1.107	0.268
GGT (U/L)	40.0 (24.8, 53.3)	30.0 (17.5, 66.0)	-1.341	0.180
ALP (U/L)	137.0 (102.0, 196.0)	130.0 (112.3, 173.0)	-0.413	0.680
ALB (g/L)	29.0 (14.6, 31.9)	26.5 (24.0, 29.6)	-1.645	0.100
TB (umol/L)	72.5 (49.7, 123.9)	75.9 (53.6, 108.6)	-0.290	0.772
TC (mmol/L)	1.9 (1.5, 2.6)	2.0 (1.8, 2.6)	-0.339	0.735
WBC (10^9/L)	4.9 (3.5, 11.0)	3.5 (2.1, 5.4)	-3.319	**0.001**
PLT (10^9/L)	82.5 (50.0, 129.8)	65.0 (42.0, 104.0)	-1.989	**0.047**
PTA (%)	46.4 (41.0, 52.8)	43.0 (37.6, 53.0)	-2.065	**0.039**
INR	1.8 (1.5, 1.9)	1.6 (1.5, 1.9)	-0.825	0.409
CTP classification, *n* (%)			0.903	0.637
Class A	1 (1.4%)	1 (1.8%)		
Class B	15 (21.4%)	16 (28.6%)		
Class C	54 (77.1%)	39 (69.6%)		
CTP score	10.0 (10.0, 12.0)	10.0 (9.0, 11.0)	-1.392	0.164
MELD score	15.8 (14.2, 20.3)	13.3 (10.5, 16.4)	-3.385	**0.001**
MELD-Na score	22.5 (15.4, 27.2)	14.8 (11.7, 18.6)	-3.975	**<0.001**
CLIF-SOFA score	12.0 (10.0, 14.0)	9.0 (7.0, 11.3)	-4.226	**<0.001**
30-day mortality	32 (45.7%)	7 (12.5%)		
90-day mortality	36 (51.4%)	9 (16.1%)		

ACLF, Acute-on-chronic liver failure; BMI, Body mass index; HBV, Hepatitis B virus; HCV, Hepatitis C virus; BUN, Blood urea nitrogen; Cr, Creatinine; Na^+, Natrium; ALT, Alanine aminotransferase; AST, Aspartate aminotransferase; GGT, Gamma-glutamyl transpeptidase; ALP, Alkaline phosphatase; ALB, Albumin; TB, Total bilirubin; TC, Total cholesterol; WBC, White blood cells; PLT, Platelet count; PTA, Prothrombin activity; INR, International normalized ratio; CTP, Child-Turcottee-Pugh; MELD, Model of end-stage liver disease; CLIF-SOFA, Chronic liver failure-sequential organ failure assessment

Spectral CT image acquisition and analysis

All participants underwent hepatic gemstone spectral CT (GE Discovery CT 750 HD, GE Healthcare, Waukesha, WI, USA) scans. Scanning parameters: the unenhanced scan was performed using the conventional helical scanning mode with a tube voltage of 120 kVp, automatic tube current modulation, a pitch of 1.375:1, a rotation speed of 0.6 s/r, and a slice thickness and increment of 1.25 mm. The contrast-enhanced scan was performed using gemstone spectral imaging (GSI) mode with a tube voltage of 80 kVp/140 kVp for instantaneous switching, and the remaining parameters were the same as for the unenhanced scan. Following the unenhanced scan, an iodinated contrast agent (Iodixanol, 320 mg/mL iodine or Iopromide, 370 mg/mL iodine) was injected at a rate of 3.5–4.0 ml/s at a dose of 1.0-1.2 ml/kg of body weight. Arterial phase (AP) scanning commenced 20 s after the abdominal aorta CT value reached 100 HU. Subsequent venous phase (VP) and equilibrium phase (EP) scans were performed at 60 s and 120 s, respectively.

All data were transferred to a workstation (GE AW4.7, GE Healthcare, Waukesha, WI, USA) and processed for analysis using GSI Volume Viewer software. The delineation of the liver regions of interest (ROI) and analysis of $ECV_{IC-liver}$ are detailed in the supplementary materials.

Measurement of L3-SMI on CT images and definition of sarcopenia

The lumbar 3 (L3)-skeletal muscle index (SMI) was derived from unenhanced CT images. Two diagnostic abdominal imaging experts, each possessing 5 years of experience, delineated the region of interest (ROI) along the skeletal muscle at the transverse processes level of L3 bilaterally. The CT value threshold (-29 ~ 150 HU) was set to obtain the cross-sectional skeletal muscle area (SMA). The average of the measurements by the two experts constituted the result, and the corresponding L3-SMI was calculated using the formula L3-SMI = SMA $(cm)^2$/height $(m)^2$ [28]. The diagnosis of sarcopenia adhered to the Japanese Society of Hepatology (JSH) guidelines for sarcopenia in liver disease: L3-SMI < 38 cm^2/m^2 in women and < 42 cm^2/m^2 in men [29].

Statistical analysis

IBM SPSS (Version 26.0; IBM, New York, USA) and R (Version 4.3.1, https://www.r-project.org/) statistical software were used for analysis. The agreement between the measured parameters of the two physicians was evaluated using intraclass correlation coefficients (ICCs), and ICCs values ≥ 0.75 were considered good. The Shapiro-Wilk normality test was performed on the measures, and the independent samples t-test was used for the measures that conformed to the normal distribution, expressed as $(\bar{\chi} \pm s)$; intergroup comparisons of measures that did not conform to the normal distribution were performed by the Mann-Whitney U-test, and expressed as M (Q1, Q3). Count data were compared using the χ^2 test or Fisher's exact test and expressed as frequency (%).

Factors influencing 90-day disease progression in ACLF patients were identified through univariate and multivariate logistic regression with a stepwise forward approach. An integrated model-nomogram, based on independent predictors, was subsequently developed. The presence of multicollinearity among variables was evaluated using the variance inflation factor (VIF), with a VIF ≥ 10 indicating a high risk of multicollinearity. Model performance was evaluated using the C-index, calibration curve, and decision curve analysis (DCA). The model's effectiveness was further assessed using the Receiver Operating Characteristic (ROC) curve and Area Under Curve (AUC). Comparative analyses were conducted against established prognostic prediction scoring models (CLIF-SOFA, MELD, MELD-Na, and CTP scores). Diagnostic efficacy was compared using Delong's test to calculate the cut-off value, sensitivity, specificity, and the AUC with Yuden's index. Statistical significance was set at two-sided $P < 0.05$.

Results

Patient characteristics

A total of 126 patients diagnosed with ACLF were included in this study, comprising 56 individuals in the stable group and 70 in the progressive group. Within the progressive group, there were 45 deaths, 18 exacerbations, and 7 liver transplants within 90 days, resulting in a disease progression rate of 55.56%. 30 patients died within 30 days (30.95%), and 45 patients died within 90 days (35.71%). The prevalence of sarcopenia, along with the counts of WBC, PLT, PTA, MELD score, MELD-Na score, and CLIF-SOFA score was higher in the progressive group, while BMI was lower compared to the stable group. All these differences achieved statistical significance ($P < 0.05$). The clinical baseline data of the patients are presented in Table 1.

L3-SMI and liver spectral CT parameters

The interobserver agreements for L3-SMI and liver spectral CT parameters, as measured by two radiologists, demonstrated good consistency, with ICC values exceeding 0.85 (Table 2). Comparative analysis of L3-SMI and equilibrium hepatic spectral CT parameters between the two ACLF patient groups revealed a significantly lower L3-SMI in the progressive group compared to the stable group. Furthermore, IC-EP, Z-EP, K_{140}-EP, NIC-EP, and $ECV_{IC-liver}$ in the progressive group were significantly elevated compared to those in the stable group (all $P < 0.05$, Table 2**and** Fig. 2). No statistically significant differences in $ECV_{IC-liver}$ scores were seen in ACLF patients

Table 2 Comparison of SMI and Liver Spectral CT parameters between two groups of patients with ACLF, along with ICC for measurements by two radiologists

SMI and liver spectral CT parameters	Progressive Group ($n=70$)	Stable Group ($n=56$)	T/U/ c^2	*P*Value	ICC
L3-SMI (cm^2/m^2)	40.5 ± 6.7	44.9 ± 5.9	3.856	**<0.001**	0.889
IC-EP (100 μg/cm^3)	20.6 (18.2, 26.1)	18.8 (16.5, 23.8)	-2.286	**0.022**	0.912
Z-EP	8.8 (8.7, 9.1)	8.7 (8.6, 8.9)	-2.298	**0.020**	0.907
K_{140}-EP	1.6 (1.5, 2.0)	1.5 (1.3, 1.8)	-2.227	**0.026**	0.913
NIC-EP	0.6 (0.5, 0.6)	0.5 (0.5, 0.6)	-3.511	**<0.001**	0.926
$ECV_{IC-liver}$	40.6 (38.8, 41.8)	31.4 (29.3, 34.8)	-6.076	**<0.001**	0.917

ACLF, Acute-on-chronic liver failure; L3-SMI, Skeletal muscle index at L3; IC, Iodine concentration; EP, Equilibrium phase; Z, Effective atomic number; K_{140}, Energy spectrum curve slope; NIC, Normalized iodine concentration; $ECV_{IC-liver}$, Extracellular liver volume; ICC, Intraclass correlation coefficient

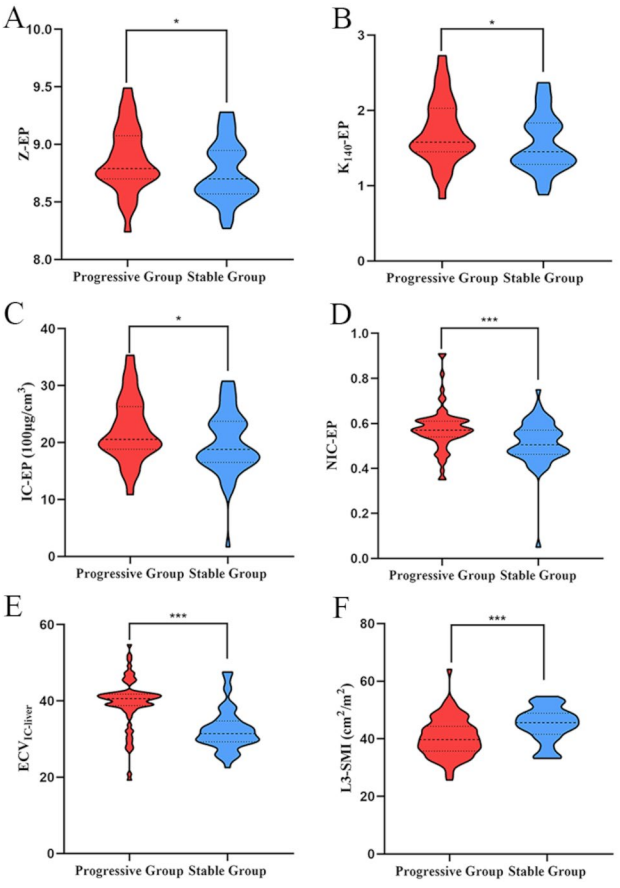

Fig. 2 Violin plots illustrating the distribution of L3-SMI and hepatic equilibrium-phase spectral CT parameters between the progressive and stable groups. EP, Equilibrium phase; Z, Effective atomic number; K_{140}, Slope of the spectral curve; IC, Iodine concentration; NIC: Normalized iodine concentration; $ECV_{IC-liver}$, Extracellular liver volume; L3-SMI: Skeletal muscle index at L3; *, $P<0.05$; ***, $P<0.001$

with different etiologies (HBV vs. Non-HBV and Alcohol vs. Non-Alcohol, Additional file 1: Table. S1). Representative images of L3-SMI and liver spectral CT for two ACLF patients are depicted in Fig. 3**and** Fig. 4.

Development and assessment of a predictive model for 90-day progression of ACLF

In the univariate analysis, BMI, WBC, PLT, PTA, L3-SMI, IC-EP, Z-EP, K_{140}-EP, NIC-EP, $ECV_{IC-liver}$, Sarcopenia, MELD-Na score, and CLIF-SOFA score demonstrated associations with disease progression status at 90 days in ACLF patients. Following the exclusion of parameters with high multicollinearity (Z-EP, K_{140}-EP, NIC-EP) using VIF, multivariate logistic regression analysis identified WBC (OR = 1.19, 95% *CI*: 1.02–1.40; $P=0.026$), $ECV_{IC-liver}$ (OR = 1.27, 95% *CI*: 1.15–1.40; $P<0.001$), Sarcopenia (OR = 4.15, 95% *CI*: 1.43–12.01; $P=0.009$), MELD-Na score (OR = 1.06, 95%*CI*: 1.01–1.13;$P=0.042$), and CLIF-SOFA score (OR = 1.37, 95%*CI*:1.15–1.64; $P<0.001$)as independent predictors of disease progression (Table 3). A predictive model for 90-day disease progression in ACLF patients was then formulated based on these three independent predictors (Fig. 5A). Each variable received a specific weight, and the cumulative score derived from all variables was directly proportional to the patient's risk of disease progression within 90 days.

The discriminative performance of the model was evaluated using the C-index, revealing a C-index of 0.910 (95% *CI*: 0.860–0.961) and a corrected C-index of 0.892. These findings indicate strong discriminative capacity in predicting disease progression status within 90 days in ACLF patients. The calibration curve closely paralleled the diagonal line, signifying excellent concordance between the model's predicted probability and actual outcomes. Additionally, the Hosmer–Lemeshow test yielded a nonsignificant *p*-value of 0.421, affirming the model's favorable fit (Fig. 5B). Results from the DCA demonstrated that the model offered greater net benefit across nearly the entire range of threshold probabilities when compared to scenarios involving all or none of the variables, underscoring its heightened clinical utility (Fig. 5C).

The performance of the proposed combined model was assessed and compared with established models (CLIF-SOFA, MELD, MELD-Na, and CTP scores). The combined model exhibited superior accuracy in predicting 90-day disease progression status in ACLF patients, boasting an AUC of 0.910 (95% *CI*: 0.860–0.961), a

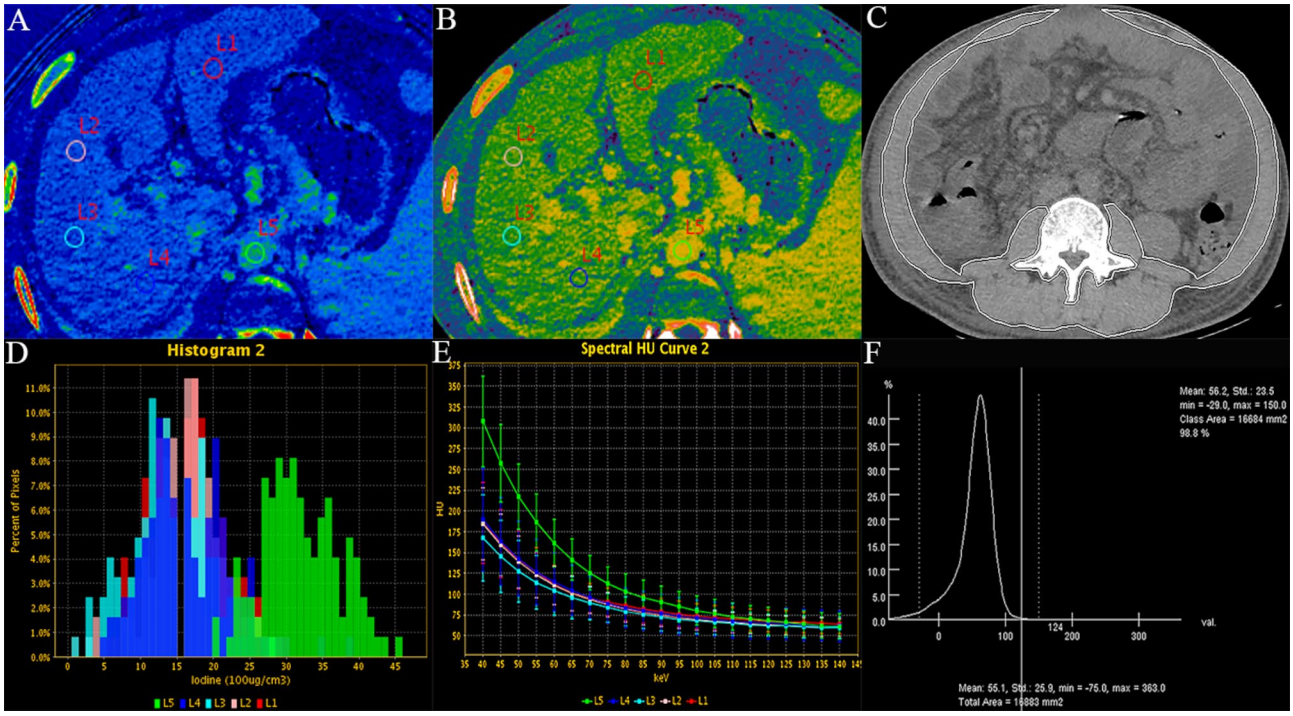

Fig. 3 (Progressive group) Equilibrium-phase liver spectral CT and L3-SMI imaging images of a 56-year-old female patient with ACLF. Panels A-F depict the iodine (water) pseudo-color map, effective atomic number map, schematic outlining skeletal muscle area (SMA), histogram, slope of the spectral curve, and SMA measurements, corresponding to IC-EP = 22.88 (100 μg/cm^3), NIC-EP = 0.57, Z-EP = 8.90, K_{140}-EP = 1.77, $ECV_{IC-liver}$ = 39.97, and L3-SMI = 35.65 (cm^2/m^2)-with sarcopenia

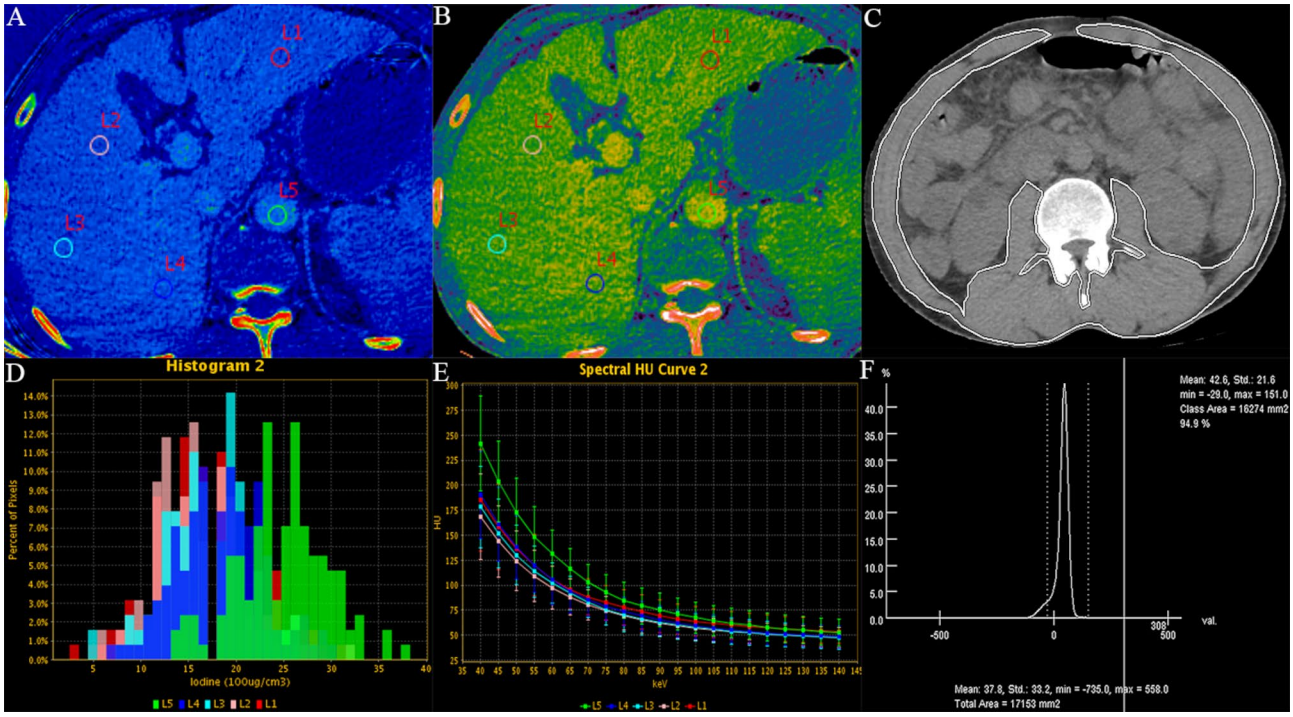

Fig. 4 (Stable group) Equilibrium-phase liver spectral CT and L3-SMI imaging images of a 60-year-old male patient with ACLF. Panels A-F depict the iodine (water) pseudo-color map, effective atomic number map, schematic outlining skeletal muscle area (SMA), histogram, slope of the spectral curve, and SMA measurements, corresponding to IC-EP = 15.63 (100 μg/cm^3), NIC-EP = 0.62, Z-EP = 8.52, K_{140}-EP = 1.20, $ECV_{IC-liver}$ = 32.88, and L3-SMI = 48.92 (cm^2/m^2)-without sarcopenia

Table 3 Univariate and Multivariate Logistic Regression Analysis for Predicting 90-Day disease progression in patients with ACLF

Variables	Univariate analysis			Multivariate analysis		
	OR	95%CI	*P*Value	OR	95%CI	*P*Value
BMI (kg/m^2)	0.93	0.84–1.02	0.115			
Sarcopenia (YES)	3.71	1.70–8.07	**<0.001**	4.15	1.43–12.01	**0.009**
WBC (10^9/L)	1.12	1.02–1.24	**0.020**	1.19	1.02–1.40	**0.026**
PLT (10^9/L)	0.99	0.98–0.99	**0.021**	1.00	0.99-1.0	0.317
PTA (%)	0.98	0.95–1.01	0.186			
L3-SMI (cm^2/m^2)	0.90	0.84–0.95	**<0.001**	1.03	0.91–1.16	0.671
IC-EP	1.08	1.01–1.15	**0.027**	1.03	0.95–1.12	0.499
$ECV_{IC-liver}$	1.22	1.13–1.31	**<0.001**	1.27	1.15–1.40	**<0.001**
MELD-Na score	1.08	1.03–1.13	**0.002**	1.06	1.01–1.13	**0.042**
CLIF-SOFA score	1.31	1.15–1.49	**<0.001**	1.37	1.15–1.64	**<0.001**

ACLF, Acute-on-chronic liver failure; BMI, Body mass index; WBC, White blood cells; PLT, Platelet count; PTA, Prothrombin activity; L3-SMI, Skeletal muscle index at L3; IC, Iodine concentration; EP, Equilibrium phase; $ECV_{IC-liver}$, Extracellular liver volume; MELD, Model of end-stage liver disease; CLIF-SOFA, Chronic liver failure-sequential organ failure assessment; OR, Odds ratio; *CI*, Confidence interval

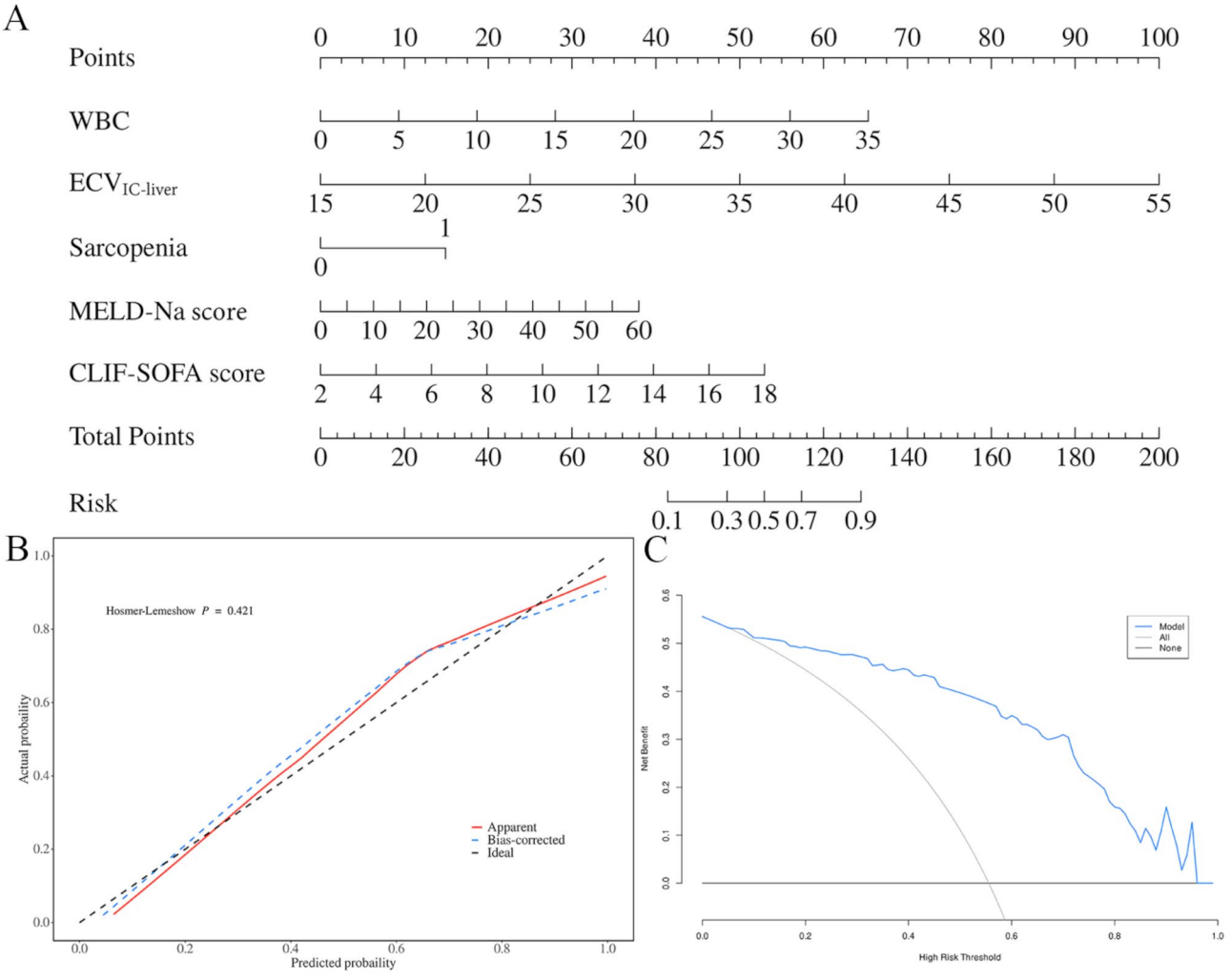

Fig. 5 Nomogram (**A**), Calibration Curve (**B**), and DCA (**C**) for Predicting 90-day Progression Status in Patients with ACLF

Table 4 Comparative analysis of ROC curves for Predicting 90-Day disease progression using clinical scores and the combined model in patients with ACLF

	AUC	95%CI	Cut-off value	Sensitivity (%)	Specificity (%)	PPV	NPV
Combined model	0.910	0.860–0.961	0.455	80.4	90.0	0.865	0.851
CLIF-SOFA score	0.719	0.629–0.809	9.517	57.1	80.0	0.696	0.700
MELD-Na score	0.707	0.613-0.800	20.588	83.9	60.0	0.627	0.824
MELD score	0.676	0.580–0.771	13.758	53.6	77.1	0.652	0.675
CTP score	0.570	0.472–0.668	9.493	30.4	81.4	0.567	0.594

CLIF-SOFA, Chronic liver failure-sequential organ failure assessment; MELD, Model for end-stage liver disease; CTP, Child-Turcottee-Pugh; AUC, Area under the curve; *CI*, Confidence interval; PPV, Positive Predictive Value; NPV, Negative Predictive Value

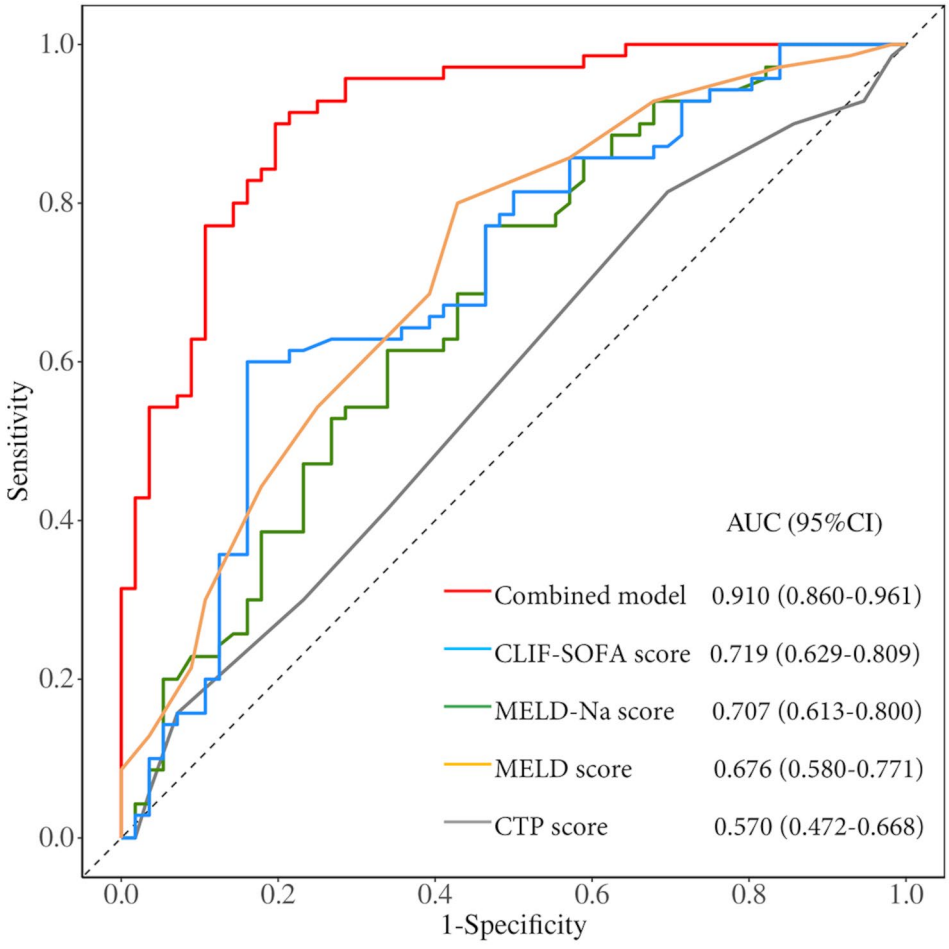

Fig. 6 Comparison of ROC Curves for Predicting 90-day Disease Progression based on Clinical Scores (CLIF-SOFA, MELD, MELD-Na and CTP scores) and the Combined Model. The AUCs was 0.910 (95% *CI*: 0.860–0.961) for the combined model, 0.719 (95% *CI*: 0.629–0.809) for CLIF-SOFA score, 0.707 (95% *CI*: 0.613-0.800) for the MELD-Na score, and 0.676 (95% CI: 0.580–0.771) for the MELD score, and 0.570 (95% *CI*: 0.472–0.668) for CTP score. The combined model demonstrated higher AUCs compared to the CLIF-SOFA, MELD, MELD-Na and CTP scores

cut-off value of 0.455, a sensitivity of 80.4%, a specificity of 90.0%, a PPV of 0.865, and an NPV of 0.851. In contrast, the AUC value for the CLIF-SOFA score was 0.719 (95% *CI*: 0.629 – 0.809), with a cutoff value of 9.517, sensitivity of 57.1%, specificity of 80.0%, PPV of 0.696, and NPV of 0.700. The AUC for the MELD-Na score was 0.707 (95% *CI*: 0.613-0.800), with a cut-off value of 20.588, a sensitivity of 83.9%, a specificity of 60.0%, a PPV of 0.627, and an NPV of 0.824. The AUC value for the MELD score was 0.676 (95% *CI*: 0.580–0.771), with a cutoff value of 13.758, sensitivity of 53.6%, specificity of 77.1%, PPV of 0.652, and NPV of 0.675. The AUC value for the CTP score was 0.570 (95% *CI*: 0.472–0.668), with a cutoff value of 9.493, sensitivity of 30.4%, specificity of 81.4%, PPV of 0.567, and NPV of 0.594 (Tables 4**and** Fig. 6). Delong's test showed that the diagnostic performance of the combined model was superior to that of

the individual clinical scores (CLIF-SOFA, MELD-Na, MELD, and CTP scores) (Additional file 1: Table S2.).

Furthermore, the combined model was used to predict 30-day and 90-day mortality in ACLF patients, with AUC values of 0.808 (95% *CI*: 0.729–0.887) and 0.825 (95% *CI*: 0.750–0.900), respectively (Additional file 1: Fig. S2).

Discussion

Prognostic accuracy plays a pivotal role in risk stratification and treatment decisions for patients with ACLF [30]. This study identified independent risk factors associated with the 90-day disease progression in ACLF patients through univariate and multivariate logistic regression analysis, including WBC (10^9/L), $ECV_{IC-liver}$ derived from the EP of spectral CT, Sarcopenia defined by L3-SMI measured with unenhanced CT, MELD-Na, and CLIF-SOFA scores. Subsequently, a combined clinical-imaging model was formulated. In comparison to existing clinical scores (CLIF-SOFA, MELD-Na, MELD, and CTP scores), the combined model, incorporating WBC, $ECV_{IC-liver}$, Sarcopenia, MELD-Na, and CLIF-SOFA scores, exhibited superior efficacy in predicting the 90-day disease progression status in ACLF patients. A visualized nomogram was developed to enhance the utility of clinical decision-making.

Evaluation of liver function is pivotal in the diagnosis and treatment of ACLF. Spectral CT, a commonly employed imaging modality for chronic liver disease, not only visually and quantitatively delineates hepatic hemodynamic changes but also yields valuable insights into liver function, particularly through the quantification of ECV derived from the EP [31]. ECV is a quantitative measure of the extracellular matrix (ECM), encompassing the intravascular space fraction and tissue interstitial space between blood vessels. It serves as an indicator of vascular growth, stromal fibrosis severity, and the cellular microenvironment, emerging as a reliable biomarker for noninvasive liver disease assessment [31, 32]. Spectral CT-derived ECV quantification offers enhanced accuracy and consistency in measuring iodine within intravascular and intervascular tissue spaces compared to conventional enhanced CT. Its superiority extends to the evaluation of hepatic fibrosis, portal hypertension, and disease progression prediction. Thus, ECV quantification by spectral CT stands out as an independent and convenient tool, less influenced by confounding factors and physiological variations, facilitating its clinical application [33, 34]. Despite these advantages, there is a paucity of clinical studies examining the prognostic value of spectral CT-derived ECV in ACLF patients. This study utilized $ECV_{IC-liver}$, quantified through spectral CT, to predict 90-day disease progression in ACLF patients. The findings underscored $ECV_{IC-liver}$ as an independent predictor of short-term progression. Notably, $ECV_{IC-liver}$ was significantly elevated in patients with an unfavorable short-term prognosis compared to those with stabilized disease, solidifying its efficacy as a predictive biomarker. Additionally, the incorporation of abdominal unenhanced CT during liver spectral CT examination allowed for the determination of L3-SMI. This parameter not only quantifies nutritional status but also provides concurrent liver-related information, presenting a more comprehensive and reliable imaging approach for evaluating the overall condition of patients.

The nutritional status of individuals with advanced liver disease constitutes a critical clinical consideration. Sarcopenia, characterized by reduced skeletal muscle mass, strength, and function, is intricately linked to the organism's nutritional well-being [35]. Numerous prior investigations have underscored that the presence of sarcopenia heightens mortality in cirrhotic patients, emphasizing the importance of regular skeletal muscle assessment in prognosis evaluation [36, 37]. Patients with advanced liver disease commonly experience increased energy expenditure (hypermetabolism), physical inactivity, ascites, and reduced energy intake due to premature satiety. These factors collectively induce hyperactivation of muscle breakdown and protein degradation systems, elevated production of proinflammatory cytokines and growth factors, impaired protein synthesis, and diuretic-induced aberrant differentiation of myoblasts. This combination of causal factors and mechanisms precipitates progressive muscle depletion, culminating in malnutrition, specifically sarcopenia [38, 39]. Our findings corroborate that sarcopenia independently predicts 90-day disease progression in ACLF patients. The hypothesized mechanism suggests a mutually reinforcing relationship between ACLF progression and sarcopenia. ACLF onset triggers the release of numerous inflammatory and growth factors, instigating disorders in muscle synthesis and regeneration. This cascade of events, coupled with heightened muscle catabolism, contributes to the malignant progression of ACLF. Consequently, sarcopenia, a prevalent complication of advanced liver disease, not only mirrors the body's nutritional status but also significantly influences disease prognosis [40].

This study establishes a correlation between elevated WBC levels and short-term adverse progression in ACLF patients, identifying WBC as an independent predictor of 90-day disease progression. Given its reflection of organismal inflammation, WBC assumes significance in ACLF pathogenesis, where an excessive inflammatory response contributes to severe tissue damage, diminishing the body's resilience and exacerbating organ failure, ultimately resulting in an unfavorable prognosis [41, 42]. Moreover, WBC serves as an indicator of immuno-nutritional status, complementing its role as an inflammation marker [43, 44]. Li F et al. [44] demonstrated a positive

correlation between WBC levels and prognostic nutritional scores, quantitatively assessing nutritional and immune status. Previous studies further affirm WBC's strong association with variceal grading and hepatic steatosis in cirrhotic patients [45, 46]. Given that ACLF patients often exhibit inflammation and malnutrition, WBC, as a marker reflecting inflammation and immunonutritional status, proves valuable in assessing poor prognosis in ACLF patients.

The CLIF-SOFA score, MELD score and MELD-Na score are widely applied prognostic models for liver disease, yet their utility in predicting outcomes in ACLF remains controversial. Recent studies, such as the one by CHANG J et al. [47], reported an underestimation of mortality by the MELD score in ACLF patients awaiting liver transplantation. Similarly, HERNAEZ R et al. [9], in a large-scale cohort study, found that the MELD-Na score predicts a lower mortality rate than the actual 90-day mortality in ACLF patients. Consequently, the MELD score and MELD-Na score exhibit limitations in assessing ACLF prognosis, possibly due to their exclusive consideration of hepatic and renal dysfunction, neglecting crucial factors like infection, nutritional status, and extrahepatic organ failure, which significantly influence ACLF prognosis [36]. The CLIF-SOFA score is a comprehensive scoring system for assessing liver and extrahepatic organ failure [11]. Therefore, we hypothesize that the CLIF-SOFA score may partially compensate for the limitations of the MELD-Na score. Therefore, this study aimed to enable early prediction of short-term disease progression in ACLF. Results indicated that WBC, Sarcopenia incidence, $ECV_{IC-liver}$, and the CLIF-SOFA and MELD-Na scores increased with disease progression, demonstrating significant intergroup differences between the two patient groups. Furthermore, a comprehensive model was devised by integrating indicators of clinical inflammation (WBC), nutritional status (Sarcopenia), hepatic ECM ($ECV_{IC-liver}$), and liver function scoring systems (CLIF-SOFA and MELD-Na scores). This combined model exhibited superior predictive efficacy compared to commonly used clinical prognostic models for liver disease (CLIF-SOFA score, MELD score, MELD-Na score, and CTP score). This finding aligns with the research conducted by PENG H et al. [7], who introduced a novel composite model named the AMPAS1 model, incorporating age, MELD score, platelet count, alpha-fetoprotein level, sarcopenia, and a combination of more than one complication. Their model demonstrated an AUC value of 0.865 for predicting 90-day adverse progression in ACLF patients. In comparison, the comprehensive model proposed in our study not only exhibits relatively better efficacy (AUC value of 0.910), but also provides easier accessibility to factors such as WBC, sarcopenia, and $ECV_{IC-liver}$. This indicates a certain clinical value in quantitatively reflecting the inflammatory condition of the organism, nutritional status, the degree of collagen and matrix protein deposition in the extracellular interstitial space of the liver, and the liver function. Specifically, the study conducted by PENG H et al. [7] involved a total of 433 patients, resulting in a lower AUC value compared to our small-sample study ($n = 126$). It is anticipated that the AUC value will further improve in the future as we conduct studies with larger sample sizes. Thus, our model serves as a reliable supplement to existing models.

This study has several limitations. Firstly, the primary aim was to identify high-risk ACLF patients with a short-term (90-day) risk of disease progression at an early stage, intending to offer a more reliable method for assessing individualized precision medical care in clinical practice. However, the study's follow-up duration was short, potentially introducing bias in the assessment of long-term prognosis. Secondly, dynamic measurements of L3-SMI were not conducted, and the relationship and mechanism between $ECV_{IC-liver}$ and L3-SMI require further exploration in subsequent studies. Lastly, this investigation was a single-center retrospective study, with patients all coming from the East Asia region. The sample size is relatively small and lacked prospective validation of the model. Future research should involve multicenter, multinational, and multi-regional collaboration, expanded sample sizes, prospective study designs, and increased internal and external validation cohorts to enhance the model's robustness. This will provide evidence-based medical insights for early prognosis prediction of ACLF, delivering a convenient, accurate, reliable, and mature prognosis prediction model for clinical diagnosis and treatment.

Conclusions

Patients without sarcopenia and/or with a lower $ECV_{IC-liver}$ have a better prognosis. The novel model introduced in this study, incorporating WBC, Sarcopenia, $ECV_{IC-liver}$, CLIF-SOFA, and MELD-Na scores demonstrated superior predictive accuracy for 90-day disease progression in patients with ACLF compared to conventional prognostic scores (CLIF-SOFA, MELD, MELD-Na, and CTP scores). This model could serve as an effective guide for the targeted and precise implementation of clinical treatment decisions.

Abbreviations

ACLF	Acute-on-chronic liver failure
CLIF-SOFA	Chronic Liver Failure-Sequential Organ Failure Assessment
$ECV_{IC-liver}$	Extracellular liver volume
EP	Equilibrium phase
L3-SMI	Skeletal muscle index at L3
IC	Iodine concentration
NIC	Normalized iodine concentration
K_{140}	Slope of the spectral curve

Z	Effective atomic number
MELD	Model for end-stage liver disease
ROC	Receiver operating characteristic
AUC	Area under the curve

Supplementary Information

The online version contains supplementary material available at https://doi.org/10.1186/s12880-025-01600-9 .

Supplementary Material 1

Acknowledgements
None.

Author contributions
Yuan Xu: Conceptualization, Validation, Formal analysis, Resources, Writing—original draft, Writing—review & editing. Fukai Li and Bo Liu: Formal analysis, Resources, Data curation, Follow up. Tiezhu Ren, Jiachen Sun, Yufeng Li and Hong Liu: Consult literatures, Statistical Analysis. Jianli Liu* and Junlin Zhou*: Conceptualization, Supervision, Project administration. All authors read and approved the final manuscript.

Funding
This study has received funding by grants of Natural Science Foundation of China (82260361, 82371914), Lanzhou University Second Hospital Second Hospital "Cuiying Technology Innovation Plan" (CY2022-QN-A10), Lanzhou University Second Hospital "Cuiying Postgraduate Instructor Cultivation Program Project (CYDSPY202003) and Outstanding Young Talents and Backbone Talents Project of Gansu Provincial Health Industry Research Program (GSWSQN2023-04).

Data availability
The data of this article can be obtained with the consent of the corresponding author.

Declarations

Ethics approval and consent to participate
The present study was approved by the ethics committee at Lanzhou University Second Hospital (No. 2022 A-112) and performed according to the ethical guidelines of the 1975 Declaration of Helsinki. The requirement for obtaining informed consent from patients was waived because of the retrospective nature of the study.

Consent for publication
Not applicable.

Competing interests
The authors declare no competing interests.

Clinical trial number
Not applicable.

Author details
[1]Department of Radiology, The Second Hospital & Clinical Medical School, Lanzhou University, Lanzhou, China
[2]Key Laboratory of Medical Imaging of Gansu Province, Lanzhou University Second Hospital, Lanzhou, China
[3]Gansu International Scientific and Technological Cooperation Base of Medical Imaging Artificial Intelligence, Lanzhou, China
[4]Department of Radiology, Second Affiliated Hospital of Navy Medical University, Shanghai, China
[5]Department of General Surgery, The Second Hospital & Clinical Medical School, Lanzhou University, Lanzhou, China

Received: 26 October 2024 / Accepted: 16 February 2025
Published online: 03 March 2025

References

1. EASL Clinical Practice Guidelines on hepatitis delta virus [J]. J Hepatol. 2023;79(2):433–60. https://doi.org/10.1016/j.jhep.2023.05.001
2. Jindal A, Sarin SK. Epidemiology of liver failure in Asia-Pacific region [J]. Liver Int. 2022;42(9):2093–109. https://doi.org/10.1111/liv.15328
3. Bernal W, Jalan R, Quaglia A, et al. Acute-on-chronic liver failure [J]. Lancet. 2015;386(10003):1576–87. https://doi.org/10.1016/S0140-6736(15)00309-8
4. Gustot T, Fernandez J. Clinical course of acute-on-chronic liver failure syndrome and effects on prognosis [J]. Hepatology. 2015;62(1):243–52. https://doi.org/10.1002/hep.27849
5. Liu C, Shen Z. Gd-BOPTA-enhanced hepatobiliary phase MR imaging can predict the prognosis of patients with acute-on-chronic liver failure [J]. Eur Radiol. 2022;32(5):3006–15. https://doi.org/10.1007/s00330-021-08440-5
6. Sarin SK, Choudhury A, Sharma M K, et al. Acute-on-chronic liver failure: consensus recommendations of the Asian Pacific association for the study of the liver (APASL): an update [J]. Hep Intl. 2019;13(4):353–90. https://doi.org/10.1007/s12072-019-09946-3
7. Peng H, Zhang Q. A prognostic model of acute-on-chronic liver failure based on sarcopenia [J]. Hepatol Int. 2022;16(4):964–72. https://doi.org/10.1007/s12072-022-10363-2
8. Reverter E, Toapanta D, Bassegoda O, et al. Critical Care Management of Acute-on-chronic liver failure: certainties and unknowns [J]. Semin Liver Dis. 2023;43(2):206–17. https://doi.org/10.1055/s-0043-1769907
9. Hernaez R, Liu Y Kramerjr, et al. Model for end-stage liver disease-sodium underestimates 90-day mortality risk in patients with acute-on-chronic liver failure [J]. J Hepatol. 2020;73(6):1425–33. https://doi.org/10.1016/j.jhep.2020.06.005
10. Abdallah M A, Kuo Y F Asranis, et al. Validating a novel score based on interaction between ACLF grade and MELD score to predict waitlist mortality [J]. J Hepatol. 2021;74(6):1355–61. https://doi.org/10.1016/j.jhep.2020.12.003
11. Liu L X, Zhang Y, Nie Y, et al. Assessing the Prediction Effect of various prognosis model for 28-Day mortality in Acute-on-chronic liver failure patients [J]. Risk Manage Healthc Policy. 2020;13:3155–63. https://doi.org/10.2147/RMHP.S281999
12. Verma N, Dhiman R K, Singh V, et al. Comparative accuracy of prognostic models for short-term mortality in acute-on-chronic liver failure patients: CAP-ACLF [J]. Hepatol Int. 2021;15(3):753–65. https://doi.org/10.1007/s12072-021-10175-w
13. Bak S, Kim J E, Bae K, et al. Quantification of liver extracellular volume using dual-energy CT: utility for prediction of liver-related events in cirrhosis [J]. Eur Radiol. 2020;30(10):5317–26. https://doi.org/10.1007/s00330-020-06876-9
14. Fahlenkamp U L, Ziegeler K, Adams L C, et al. Intracellular accumulation capacity of gadoxetate: initial results for a novel biomarker of liver function [J]. Sci Rep. 2020;10(1):18104. https://doi.org/10.1038/s41598-020-75145-y
15. Xu Y, Li Y, Li S, Xue S, Liu J. Dual-energy CT quantification of extracellular liver volume predicts short-term disease progression in patients with hepatitis B liver cirrhosis-acute decompensation. Insights Imaging. 2023;14(1):51. Published 2023 Mar 29. https://doi.org/10.1186/s13244-023-01393-x
16. Topan MM, Sporea I, Dănilă M, et al. Impact of Sarcopenia on Survival and clinical outcomes in patients with liver cirrhosis [J]. Front Nutr. 2021;8:766451. https://doi.org/10.3389/fnut.2021.766451
17. Zhou D, Zhang D, Zeng C, et al. Impact of Sarcopenia on the survival of patients undergoing liver transplantation for decompensated liver cirrhosis [J]. J Cachexia Sarcopenia Muscle. 2023. https://doi.org/10.1002/jcsm.13334
18. Zeng F, Jiang W, Chang X, et al. Sarcopenia is associated with short- and long-term mortality in patients with acute-on-chronic liver failure [J]. J Cachexia Sarcopenia Muscle. 2024;15(4):1473–82. https://doi.org/10.1002/jcsm.13501
19. Dasarathy S, Merli M. Sarcopenia from mechanism to diagnosis and treatment in liver disease [J]. J Hepatol. 2016;65(6):1232–44. https://doi.org/10.1016/j.jhep.2016.07.040
20. Dajti E, Rodrigues SG. Sarcopenia evaluated by EASL/AASLD computed tomography-based criteria predicts mortality in patients with cirrhosis: a systematic review and meta-analysis [J]. JHEP Rep. 2024;6(8):101113. https://doi.org/10.1016/j.jhepr.2024.101113
21. Jiang M, Hua X, Wu M, et al. Longitudinal changes in Sarcopenia was associated with survival among cirrhotic patients [J]. Front Nutr. 2024;11:1375994. https://doi.org/10.3389/fnut.2024.1375994
22. Shi Z W Zengx. Sarcopenia as a prognostic predictor of liver cirrhosis: a multicentre study in China [J]. J Cachexia Sarcopenia Muscle. 2021;12(6):1948–58. https://doi.org/10.1002/jcsm.12797

23. Chianca V, Albano D, Messina C, et al. Sarcopenia: imaging assessment and clinical application. Abdom Radiol (NY). 2022;47(9):3205–16. https://doi.org/10.1007/s00261-021-03294-3
24. Bai J, Xu M, Peng F, et al. Skeletal muscle mass index as a predictor of long-term cirrhosis onset in young non-cirrhotic males with acute-on-chronic liver failure [J]. Front Nutr. 2022;9:1071373. https://doi.org/10.3389/fnut.2022.1071373
25. Sarin SK, Choudhury A, Sharma M K, et al. Acute-on-chronic liver failure: consensus recommendations of the Asian Pacific association for the study of the liver (APASL): an update [J]. Hepatol Int. 2019;13(4):353–90. https://doi.org/10.1007/s12072-019-09946-3
26. Moreau R, Jalan R, Gines P, et al. Acute-on-chronic liver failure is a distinct syndrome that develops in patients with acute decompensation of cirrhosis [J]. Gastroenterology. 2013;144(7):1426–e143714379. https://doi.org/10.1053/j.gastro.2013.02.042
27. Lee S K, Song M J, Kim SH, et al. Comparing various scoring system for predicting overall survival according to treatment modalities in hepatocellular carcinoma focused on platelet-albumin-bilirubin (PALBI) and albumin-bilirubin (ALBI) grade: a nationwide cohort study [J]. PLoS ONE. 2019;14(5):e0216173. https://doi.org/10.1371/journal.pone.0216173
28. Koya S, Kawaguchi T, Hashida R, et al. Effects of in-hospital exercise on Sarcopenia in hepatoma patients who underwent transcatheter arterial chemoembolization [J]. J Gastroenterol Hepatol. 2019;34(3):580–8. https://doi.org/10.1111/jgh.14538
29. Nishikawa H, Shiraki M. Japan Society of Hepatology guidelines for Sarcopenia in liver disease (1st edition): recommendation from the working group for creation of Sarcopenia assessment criteria [J]. Hepatol Res. 2016;46(10):951–63. https://doi.org/10.1111/hepr.12774
30. Jalan R, Gustot T, Fernandez J, et al. Equity' and 'Justice' for patients with acute-on chronic liver failure: a call to action [J]. J Hepatol. 2021;75(5):1228–35. https://doi.org/10.1016/j.jhep.2021.06.017
31. Peng Y, Tang H, Huang Y, et al. CT-derived extracellular volume and liver volumetry can predict posthepatectomy liver failure in hepatocellular carcinoma [J]. Insights Imaging. 2023;14(1):145. https://doi.org/10.1186/s13244-023-01496-5
32. Ozaki K, Ohtani T, Ishida T, et al. Liver fibrosis estimated using extracellular volume fraction obtained from dual-energy CT as a risk factor for hepatocellular carcinoma after sustained virologic response: a preliminary case-control study [J]. Eur J Radiol. 2023;168:111112. https://doi.org/10.1016/j.ejrad.2023.111112
33. Nagayama Y, Kato Y, Inoue T, et al. Liver fibrosis assessment with multiphasic dual-energy CT: diagnostic performance of iodine uptake parameters [J]. Eur Radiol. 2021;31(8):5779–90. https://doi.org/10.1007/s00330-021-07706-2
34. Kim J E Hongs, Cho JM, et al. Quantification of liver extracellular volume using dual-energy CT for ruling out high-risk varices in cirrhosis [J]. Eur J Radiol. 2022;148:110151. https://doi.org/10.1016/j.ejrad.2022.110151
35. Wu Y K, Li M, Zhang YC, et al. The Sarcopenia index is an effective predictor for malnutrition in patients with liver cirrhosis [J]. Nutr Dietetics: J Dietitians Association Australia. 2022;79(5):563–71. https://doi.org/10.1111/1747-0080.12738
36. Kang SH, Jeong W K, Baik SK, et al. Impact of Sarcopenia on prognostic value of cirrhosis: going beyond the hepatic venous pressure gradient and MELD score [J]. J Cachexia Sarcopenia Muscle. 2018;9(5):860–70. https://doi.org/10.1002/jcsm.12333
37. Liu J, Ma J, Yang C, et al. Sarcopenia in patients with cirrhosis after Transjugular Intrahepatic Portosystemic Shunt Placement [J]. Radiology. 2022;303(3):711–9. https://doi.org/10.1148/radiol.211172
38. Puchades Renau L, Herreras López J, Cebrià I I M, et al. Frailty and Sarcopenia in Acute-on-chronic liver failure [J]. Hepatol Commun. 2021;5(8):1333–47. https://doi.org/10.1002/hep4.1722
39. Marasco G, Dajti E, Ravaioli F, et al. Clinical impact of Sarcopenia assessment in patients with liver cirrhosis [J]. Expert Rev Gastroenterol Hepatol. 2021;15(4):377–88. https://doi.org/10.1080/17474124.2021.1848542
40. He Y, Hu L. Nutritional screening and assessment tools for patients with cirrhosis based on the Global Leadership Initiative on Malnutrition criteria [J]. J Hum Nutr Diet. 2023. https://doi.org/10.1111/jhn.13265
41. Moreau R. The pathogenesis of ACLF: the inflammatory response and Immune function [J]. Semin Liver Dis, 2016, 36(2): 133–40. https://doi.org/10.1055/s-0036-1583199
42. Jachs M, Hartl L, Schaufler D, et al. Amelioration of systemic inflammation in advanced chronic liver disease upon beta-blocker therapy translates into improved clinical outcomes [J]. Gut. 2021;70(9):1758–67. https://doi.org/10.1136/gutjnl-2020-322712
43. Forget P, Echeverria G, Giglioli S, et al. Biomarkers in immunonutrition programme, is there still a need for new ones? A brief review [J]. Ecancermedicalscience. 2015;9:546. https://doi.org/10.3332/ecancer.2015.546
44. Li F, Li C, Sun Y, et al. Cerebral ischemic complications after Surgical revascularization for Moyamoya Disease: risk factors and development of a predictive model based on Preoperative Nutritional Blood parameters [J]. Front Nutr. 2022;9:842838. https://doi.org/10.3389/fnut.2022.842838
45. Bayani A, Hosseini A, Asadi F, et al. Identifying predictors of varices grading in patients with cirrhosis using ensemble learning [J]. Clin Chem Lab Med. 2022;60(12):1938–45. https://doi.org/10.1515/cclm-2022-0508
46. Sung KT, Kuo R, Sun JY, et al. Associations between CT-determined visceral fat burden, hepatic steatosis, circulating white blood cell counts and neutrophil-to-lymphocyte ratio [J]. PLoS ONE. 2018;13(11):e0207284. https://doi.org/10.1371/journal.pone.0207284
47. Chang J, Matheja A, Krzycki S et al. Model for end-stage liver disease underestimates mortality of patients with acute-on-chronic liver failure waiting for liver transplantation [J]. Digestive and liver disease: official journal of the Italian Society of Gastroenterology and the Italian Association for the study of the liver, 2022, 54(6): 784–90. https://doi.org/10.1016/j.dld.2021.12.011

Publisher's note